HadSST.4.1.0.0 release notes

Caroline Sandford

February 2025

1 Overview

HadSST.4.1.0.0 is a minor release of the HadSST dataset that replaces HadSST.4.0.1.0. There have been no changes to the science in this release, which remains as documented by Kennedy et al. (2019). However, significant technical changes have been implemented including:

- Complete re-implementation of the HadSST system in Python (previously IDL)
- Addition of unit testing and stricter version control / QA procedures (GitHub)
- Move from manual to automated workflows (implemented in Cylc 8)

The product offering has also been slightly reduced, to remove additional uncertainty components that are not necessary for the propagation of uncertainties through calculations such as regional averaging.

The process of re-implementation has changed some aspects of the HadSST ensemble in expected ways, through changes in numerical optimisation behaviour between Python and IDL, and from the new random seeds used to generate perturbed parameters for the ensemble. Some bugs were also discovered in the HadSST.4.0.1.0 IDL code, which have been fixed in this release. The magnitude of the resulting changes to global average SST anomalies is small and falls well within the expected uncertainty range.

The key differences between HadSST.4.1.0.0 and HadSST.4.0.1.0 are:

- Changes to the random seeds used to generate parameters for the ensemble
- Minor bug fixes to the calculation of pre-1941 bucket bias corrections and of coverage uncertainty for timeseries products
- Changes to spatial ancillaries affecting the spatial pattern of post-1945 bias corrections
- Extension to temporal smoothing of modern engine room intake (ERI) bias corrections
- Bug fixes to “fraction of correct metadata” estimation, affecting the inferred timing of the transition to modern insulated buckets and overall bias corrections between 1945 and 1980

In addition, some changes to input data filtering were introduced in January 2022 that have not been previously documented, and so are included in these release notes. Further details are provided in section 2. The impact on global mean temperature timeseries, including graphical comparison with ERSSTv6, is shown in section 3.

2 Details of changes

2.1 Input data filtering (since January 2022)

In January 2022 the input data feed for HadSST.4.0.1.0 was switched from ICOADS to a combination of near-real-time in-situ ocean observations from the Copernicus Marine Data Service [1], Met Office GTS data and moored buoy data from IQUAM [2] (Xu and Ignatov, 2014). This led to the implementation of automated filtering to remove observations with large relative biases. Per-platform bias estimation is performed on each month of data using the procedure documented in (Kennedy et al., 2019, appendix A3.2), and observations from platforms with relative biases greater than ± 1°C are excluded from further processing. This procedure has been replicated in HadSST.4.1.0.0 and is applied to all data from January 2022 onwards.

2.2 Minor bug fixes

Two minor bug fixes have been applied in HadSST.4.1.0.0. First: following Rayner et al. (2006), data from HadNMAT2 are used in estimating some pre-1941 bucket bias corrections. A previous HadSST version had a data mask incorrectly applied to HadNMAT2, affecting bucket bias corrections for half of the ensemble members. This has been fixed in HadSST.4.1.0.0.

A second fix has been applied to the calculation of coverage uncertainty for regional average time-series. HadSST3 used the standard deviation of differences of subsampled averages from a spatially complete field to represent coverage uncertainty (Kennedy et al., 2011a). The intent was to update this in HadSST.4.0.0.0 to use the RMS difference, which reflects that the error in a regional average based on a spatially incomplete field may not be unbiased; this increases the coverage error for each region. However, this was not implemented at the time. The update to use RMS differences has now been implemented in HadSST.4.1.0.0.

2.3 Spatial pattern of bias corrections

Following earlier versions of HadSST4, HadSST.4.1.0.0 uses an interpolation method based on Karspeck et al. (2012) to estimate grid-point biases in ERI and modern insulated bucket measurements (Kennedy et al., 2019, appendix A2). These calculations rely on estimates of the spatial covariance of SSTs following the method described in Kennedy et al. (2019), appendix A1. The estimates of length scale informing these covariances are established via a cost function minimisation using detrended SSTs from ARC satellite observations (Merchant et al., 2012).

The temporal fitting and detrending applied in python for HadSST.4.1.0.0 produces quantitatively different outputs than IDL. The IDL "AMOEBA" routine used for the fitting in HadSST.4.0.1.0 is known to be approximate, and often produces detrended SSTs with non-zero residuals. However, the outputs from the python routine are much smoother spatially, leading to significantly longer estimated decorrelation length scales and spatial covariances.

The changes to spatial covariance have no impact on global, tropical (20°S-20°N) or hemispherical SST averages in HadSST.4.1.0.0. Some impacts, however, can be seen in the local pattern of bias corrections since WW2, particularly in the 1960s and 1970s where ERI biases dominate. This

[1] https://doi.org/10.48670/moi-00036

[2] https://www.star.nesdis.noaa.gov/socd/sst/iquam

may therefore have an impact on local SST timeseries for small regions. Further work on spatial covariance estimation is planned for a future HadSST release.

2.4 Temporal smoothing of ERI biases

Before application to correct SSTs, ERI biases are smoothed in time at the grid-point scale using a 5-year LOESS smoothing window (Kennedy et al., 2019). In HadSST.4.0.1.0 this window was truncated after 2018, with data after that point being smoothed backwards in time only, to ensure reproducibility of the dataset each month. For HadSST.4.1.0.0 the two-way temporal smoothing has been extended to the end of 2023, and the ongoing one-way smoothing extended to achieve a less noisy updating timeseries.

2.5 Transition to modern insulated buckets

Post-war SST measurement bias estimates are dependent on the timing of the transition from uninsulated canvas to insulated rubber buckets. Kennedy et al. (2019) describe a method of estimating both the fraction of canvas buckets and the "fraction of correct metadata" (the proportion of measurements assigned to "bucket" type that were actually from buckets) for HadSST4 by comparing the analysed biases of subsets of the input observations (ship, ERI and bucket). Realistic bounds on the parameters inferred from this calculation are used to generate a set of physically plausible dates for the start and end of the canvas-to-rubber bucket transition, from which the ensemble is sampled. The dates determined in HadSST.4.0.1.0 are shown in the left-hand panel of figure 1, published as figure 7c in Kennedy et al. (2019).

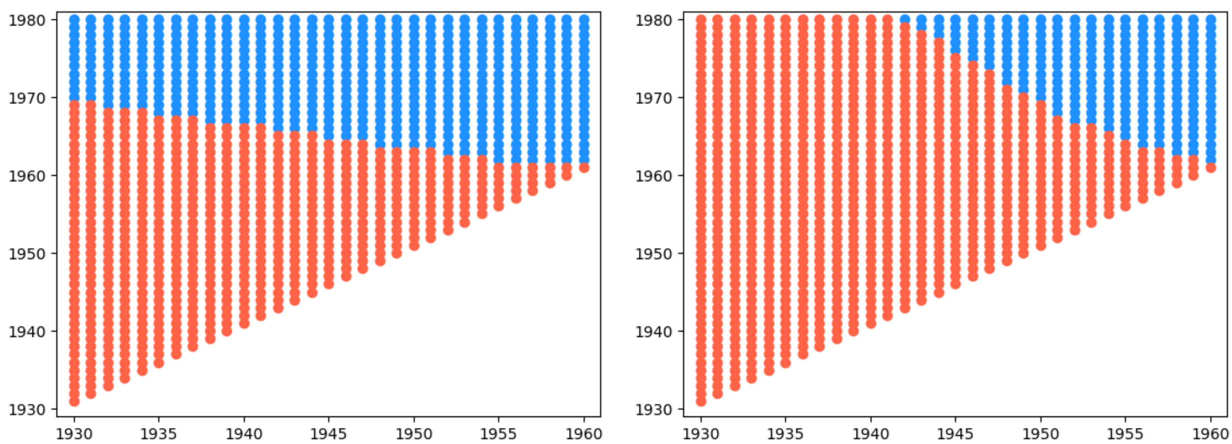

Figure 1: Accepted (blue) and rejected (red) pairs of start (x-axis) and end (y-axis) years for the canvas to rubber bucket transition. Left: reproduction of figure 7c from Kennedy et al. (2019). Right: transition dates estimated in HadSST.4.1.0.0.

The original implementation of this procedure was found to have a number of bugs, which have been fixed in HadSST.4.1.0.0. This leads to a more restricted subset of start and end dates for the canvas-to-rubber bucket transition (figure 1, right-hand panel), and places the start of the transition significantly later than in HadSST.4.0.1.0.

Although the impact on the global mean temperature record is minimal, this change is physically meaningful and merits consideration in a wider context. The figure published in Kennedy et al. (2019) suggests insulated rubber buckets could have been introduced as early as the 1930s, while the updated figure has no plausible start dates prior to 1942. Both figures agree on an end date to the transition between 1960 and 1980.

Dating the canvas-to-rubber bucket transition is a niche question in the literature, which is typically treated only in passing if mentioned at all. The most thorough discussion of this issue is found in Kennedy et al. (2011b), which presents a brief review of guidelines on measurement practises provided by several national meteorological agencies dating from the 1920s to the mid-1980s. Based on this review, the authors date the most likely start of the canvas-to-rubber bucket transition as between 1954 and 1957. This is in agreement with other literature available at the time (eg Kent et al., 2010; Kent and Taylor, 2006; Folland and Parker, 1995), which consistently refer to a mixture of canvas and wooden buckets prior to 1941, with no reference to modern insulated buckets being introduced before 1945.

Some empirical estimates of the canvas-to-rubber bucket transition are referred to in more recent literature. Hirahara et al. (2014) implement a similar calculation to Kennedy et al. (2019) to estimate the fractions of uninsulated (canvas) bucket measurements in COBE-SST2 between 1942 and 2010. While the exact dates for the transition are not reported, the authors find that uninsulated bucket biases dominate the overall bias estimate prior to 1960, suggesting a significant fraction of canvas buckets were still being used until this time. Carella et al. (2018) also find evidence that canvas bucket biases dominated overall SST bias until the 1960s. Notably, although a thorough review was conducted, no evidence or reference was found in the existing literature to the widespread introduction of insulated buckets prior to the Second World War. Thus, the corrected implementation in HadSST.4.1.0.0 produces a result that is more consistent with existing literature than that published in Kennedy et al. (2019).

3 Impact on global averages

The changes to the evolution of global mean SSTs from HadSST.4.0.1.0 to 4.1.0.0 are minimal. Figure 2 shows the difference in annual global mean SST anomaly timeseries between HadSST.4.1.0.0 and HadSST.4.0.1.0 in the context of their known uncertainties. These uncertainties include those

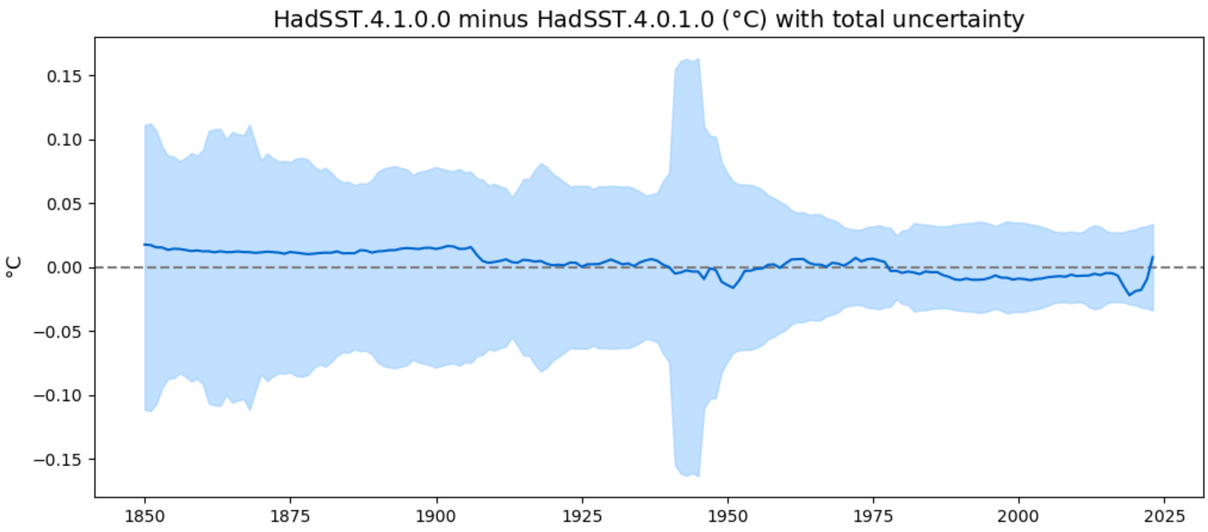

Figure 2: Annual median difference in global mean SST anomaly (°C) between HadSST.4.1.0.0 and HadSST.4.0.1.0. Shading shows total uncertainty for the HadSST.4.1.0.0 global mean.

related to correlated and uncorrelated measurement errors, sampling uncertainty (related to the distribution of observations within each grid cell), coverage uncertainty (related to the grid cells contributing to a spatial average) and uncertainty on the bias correction (represented by the spread of the ensemble). This total uncertainty range is shown by the shading in figure 2.

Although very small in the context of the estimated uncertainties, these median differences are of order 0.01°C, which may be of interest to some users. Specific features can be explained as follows:

- The increase in anomaly prior to 1910 is due to fixing the HadNMAT2 masking bug and its impact on early bucket bias corrections.
- The feature towards the end of the timeseries (2019-2024) is due to the two-way temporal smoothing of ERI biases being extended beyond the end of 2018.
- Slight changes in shape of the timeseries between 1945 and 1980 are due to the fixes to "fraction of correct metadata" and the inferred transition between canvas and rubber buckets, which has a corresponding impact on bias corrections.
- The increase in the estimated proportion of canvas buckets between 1945 and 1980 causes a slight warming of bias-corrected SSTs over the climatology period (1961-1990). This leads the whole timeseries to be shifted very slightly downward when it is re-baselined, which is responsible for the offset since the 1980s.
- Smaller scale fluctuations are due to changes in random seeds across several parameter estimation steps that use reproducible random sampling (see Kennedy et al., 2019, for details).

Figure 3 shows the global average SST anomaly timeseries for the two HadSST versions with their respective total uncertainties, compared to the global mean of the recently released ERSSTv6 dataset (Huang et al., 2024, 2017). ERSST has been re-baselined to a 1961-1990 climatology to match HadSST. This further illustrates that compared to the differences between the HadSST and ERSST datasets and the uncertainty ranges, the overall difference between HadSST.4.1.0.0 and HadSST.4.0.1.0 is negligible.

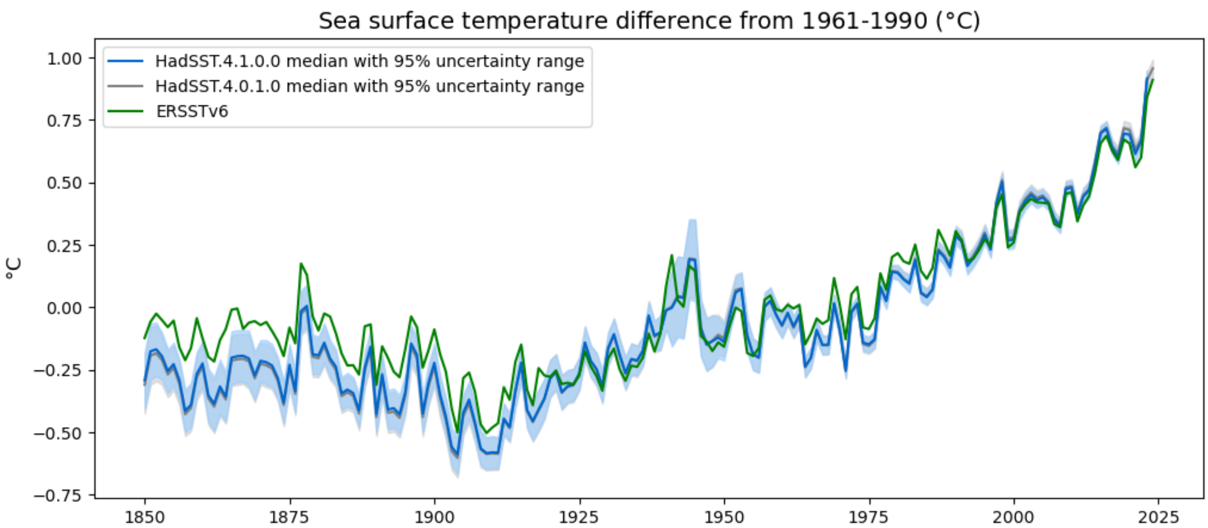

Figure 3: Annual global mean SST anomaly (°C relative to 1961-1990) timeseries compared with data from ERSSTv6. Shading shows the 95% uncertainty range representing measurement, sampling, coverage and bias correction uncertainty for HadSST.4.1.0.0 and HadSST.4.0.1.0.

References

Carella, G., J. J. Kennedy, D. I. Berry, S. Hirahara, C. J. Merchant, S. Morak-Bozzo, and E. C. Kent, 2018: Estimating Sea Surface Temperature Measurement Methods Using Characteristic Differences in the Diurnal Cycle. *Geophysical Research Letters*, **45 (1)**, 363–371, doi:https://doi.org/10.1002/2017GL076475.

Folland, C. K. and D. E. Parker, 1995: Correction of instrumental biases in historical sea surface temperature data . *Quarterly Journal of the Royal Meteorological Society*, **121**, 319–367, doi:https://doi.org/10.1002/qj.49712152206.

Hirahara, S., M. Ishii, and Y. Fukuda, 2014: Centennial-scale sea surface temperature analysis and its uncertainty. *Journal of Climate*, **27 (1)**, 57–75, doi:https://doi.org/10.1175/JCLI-D-12-00837.1.

Huang, B., et al., 2017: Extended Reconstructed Sea Surface Temperature, Version 5 (ERSSTv5): Upgrades, Validations, and Intercomparisons. *Journal of Climate*, **30 (20)**, 8179–8205, doi:https://doi.org/10.1175/JCLI-D-16-0836.1.

Huang, B., et al., 2024: A Data Upgrade for The Extended Reconstructed Sea Surface Temperature Version 6 (ERSSTv6). *2024 Ocean Sciences Meeting*, AGU.

Karspeck, A. R., A. Kaplan, and S. R. Sain, 2012: Bayesian modelling and ensemble reconstruction of mid-scale spatial variability in North Atlantic sea-surface temperatures for 1850–2008 . *Quarterly Journal of the Royal Meteorological Society*, **138 (662)**, 234–248, doi:https://doi.org/10.1002/qj.900.

Kennedy, J. J., N. A. Rayner, C. P. Atkinson, and R. E. Killick, 2019: An Ensemble Data Set of Sea Surface Temperature Change From 1850: The Met Office Hadley Centre HadSST.4.0.0.0 Data Set . *Journal of Geophysical Research: Atmospheres*, **124**, 7719–7763, doi:https://doi.org/10.1029/2018JD029867.

Kennedy, J. J., N. A. Rayner, R. O. Smith, D. E. Parker, and M. Saunby, 2011a: Reassessing biases and other uncertainties in sea surface temperature observations measured in situ since 1850: 1. Measurement and sampling uncertainties . *Journal of Geophysical Research: Atmospheres*, **116 (D14)**, doi:https://doi.org/10.1029/2010JD015218.

Kennedy, J. J., N. A. Rayner, R. O. Smith, D. E. Parker, and M. Saunby, 2011b: Reassessing biases and other uncertainties in sea surface temperature observations measured in situ since 1850: 2. Biases and homogenization . *Journal of Geophysical Research: Atmospheres*, **116**, doi:https://doi.org/10.1029/2010JD015220.

Kent, E. C., J. J. Kennedy, D. I. Berry, and R. O. Smith, 2010: Effects of instrumentation changes on sea surface temperature measured in situ. *WIREs Climate Change*, **1 (5)**, 718–728, doi:https://doi.org/10.1002/wcc.55.

Kent, E. C. and P. K. Taylor, 2006: Toward Estimating Climatic Trends in SST. Part I: Methods of Measurement . *Journal of Atmospheric and Oceanic Technology*, **23 (3)**, 464–475, doi:https://doi.org/10.1175/JTECH1843.1.

Merchant, C. J., et al., 2012: A 20 year independent record of sea surface temperature for climate from Along-Track Scanning Radiometers . *Journal of Geophysical Research: Oceans*, **117 (C12)**, doi:https://doi.org/10.1029/2012JC008400.

Rayner, N. A., P. Brohan, D. E. Parker, C. K. Folland, J. J. Kennedy, M. Vanicek, T. J. Ansell, and S. F. B. Tett, 2006: Improved Analyses of Changes and Uncertainties in Sea Surface Temperature Measured In Situ since the Mid-Nineteenth Century: The HadSST2 Dataset . *Journal of Climate*, **19**, 446–469, doi:https://doi.org/10.1175/JCLI3637.1.

Xu, F. and A. Ignatov, 2014: In situ SST Quality Monitor (iQuam). *Journal of Atmospheric and Oceanic Technology*, **31 (1)**, 164–180, doi:https://doi.org/10.1175/JTECH-D-13-00121.1.